Title
Composite material made of plasmonic nanoshells with quantum dot cores: loss-compensation and ε-near-zero physical properties

Journal
Nanotechnology, 23(23)

ISSN
0957-4484

Authors
Campione, Salvatore
Capolino, Filippo

Publication Date
2012-06-15

DOI
10.1088/0957-4484/23/23/235703

Nanotechnology **23** (2012) 235703 (6pp) doi:10.1088/0957-4484/23/23/235703

Composite material made of plasmonic nanoshells with quantum dot cores: loss-compensation and ε-near-zero physical properties

Salvatore Campione and Filippo Capolino[1]

Department of Electrical Engineering and Computer Science, University of California Irvine, CA 92697-2625, USA

E-mail: f.capolino@uci.edu

Received 27 March 2012
Published 17 May 2012
Online at stacks.iop.org/Nano/23/235703

Abstract

A theoretical investigation of loss-compensation capabilities in composite materials made of plasmonic nanoshells is carried out by considering quantum dots (QDs) as the nanoshells' cores. The QD and metal permittivities are modeled according to published experimental data. We determine the modes with real or complex wavenumber able to propagate in a 3D periodic lattice of nanoshells. Mode analysis is also used to assess that only one propagating mode is dominant in the composite material whose optical properties can hence be described via homogenization theory. Therefore, the material effective permittivity is found by comparing different techniques: (i) the mentioned mode analysis, (ii) Maxwell Garnett mixing rule and (iii) the Nicolson–Ross–Weir method based on transmission and reflection when considering a metamaterial of finite thickness. The three methods are in excellent agreement, because the nanoshells considered in this paper are very subwavelength, thus justifying the parameter homogenization. We show that QDs are able to provide loss-compensated ε-near-zero metamaterials and also loss-compensated metamaterials with large negative values of permittivity. Besides compensating for losses, the strong gain via QD can provide optical amplification with particular choices of the nanoshell and lattice dimensions.

(Some figures may appear in colour only in the online journal)

1. Introduction

In this paper we investigate the optical properties arising from composite materials made of plasmonic nanoshells. A comprehensive way to understand and classify collective resonances in such composite materials is by modal analysis [1–3] of a three-dimensional (3D) periodic structure as in figure 1. In particular, under certain circumstances of polarization and excitation, a 3D periodic lattice of plasmonic nanoshells with finite thickness could be described to a good approximation as a homogeneous slab with effective parameters, such as relative permittivity (ε_{eff}) and refractive index (n_{eff}). This effective medium representation allows for the generation of interesting physical properties at specific frequency bands, e.g. ε-near-zero (ENZ) metamaterials [4], cloaking [5] and 'perfect lenses' [6]. However, the metamaterial performance is usually affected and highly limited by the presence of large absorption losses. Therefore, loss-compensation mechanisms are inherently required to overcome this issue. Recently, active photonic materials such as fluorescent dye molecules, rare earth materials or quantum dots (QDs) have been proposed as a promising solution, because the gain experienced through the stimulated emission of an active medium is capable

[1] http://capolino.eng.uci.edu.

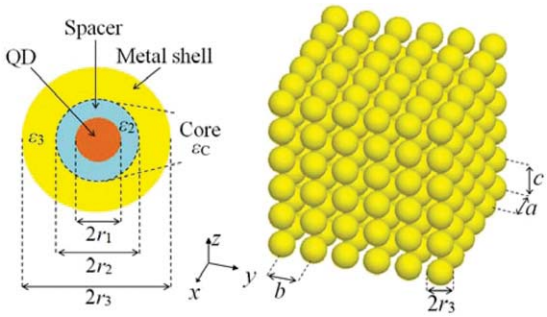

Figure 1. Composite material made of a 3D periodic lattice of nanoshells embedded in a homogeneous medium with relative permittivity ε_h. Each nanoshell core is a QD plus a spacer. The shell is made of metal. The QD internal radius is r_1, the spacer has outer radius r_2, with relative permittivity ε_2, the shell has outer radius r_3, with relative permittivity ε_3; a, b and c are the periodicities along x, y and z directions, respectively. We assume the nanoshell core has a radius r_2 and an equivalent relative permittivity ε_C.

of counteracting the high absorption losses. Dye molecules have, in general, lower emission and absorption cross sections than other active materials (e.g. QDs employed here). Moreover, high molecular concentration may diminish the overall compensation due to fluorescence quenching and/or other non-radiative phenomena [7]. Quantum dots usually have large cross sections and their emission frequency can be adjusted by modifying their physical dimensions: the smaller the radius of the QD, the larger the emission frequency [8, 9].

This characteristic greatly eases the design of loss-compensated metamaterials since one of the physical properties required for an effective loss-compensation is the 'spectrum overlap': the metamaterial physical dimensions have to be chosen such that the optical properties of interest arise at a frequency region that overlaps, at least partly, with the emission spectrum of the adopted gain material. Here, we consider QDs as the nanoshells' cores in 3D periodic lattices of such nanoparticles as in figure 1 and generate loss-compensated ENZ metamaterials and also loss-compensated metamaterials with large negative values of permittivity. Optical loss-compensation has recently been the focus of many published works, from both the experimental and theoretical points of view. Experimentally, Coumarin C500 and Rhodamine 6G fluorescent dyes, embedded into the dielectric shell of randomly dispersed nanoshells, have been used to mitigate the absorption at optical frequencies in [10, 11]. Similarly, in [12], Rhodamine 800 dyes have been used in the fishnet structure, and the experimental results, along with numerical simulations, demonstrated that the fabricated sample was loss-compensated. Theoretically, homogenized effective parameters of metamaterials made of nanoshells have been analyzed in [13], where ideal loss/gain conditions have been set through the imaginary part of the dielectric cores. A binary mixture of two kinds of QDs [8, 14], as well as of QDs and silver nanorods [15, 16], has shown the feasibility of lossless negative effective permittivity. A near-infrared ENZ metamaterial has been shown in [17] by using QDs in the nanoshells' cores. Similar structures have been used in [18] to obtain loss-compensated negative permittivity at near-infrared. Realistic parameters of dye molecules (specifically Rhodamine 6G and Rhodamine 800) have been used in [3] to compensate for the losses in 3D periodic lattices of nanoshells, focusing on the generation of an ENZ metamaterial at optical frequencies. Here, besides using QDs instead of dye molecules as in [3], we also compare theoretical results, based on complex mode analysis, with full-wave electromagnetic simulation ones. There is still a lack of understanding regarding the usage of QDs for loss-compensation capabilities and on the possibility of using effective material parameters; thus, this paper aims at providing some physical insights.

2. Modes in the composite material

The nanoshells' cores are assumed to be made of CdSe QDs surrounded by spacers (see figure 1) with matched relative permittivity ε_2 to avoid surface polarization screening charge [8, 19]. Assume then that the QD can be optically pumped to gain condition, such that the equivalent dielectric function ε_C of QD and spacer in the presence of gain, assumed to be homogeneous because $r_2 \ll \lambda_{0,\min}$, with $\lambda_{0,\min}$ the minimum free space wavelength, is calculated using the formalism in [8, 19, 20]. Accordingly

$$\varepsilon_C = \varepsilon_2 + \frac{S\omega_e^2}{\omega^2 - \omega_e^2 + i2\omega\gamma_{QD}}, \tag{1}$$

where $\omega_e = 2\pi f_e$, $f_e = 604$ THz is the emission frequency, $\gamma_{QD} = 6.07 \times 10^{13}$ s^{-1} is the broadening parameter, $S = 0.53$ the unitless transition strength and $\varepsilon_2 = 10.2$ (values taken from [8, 21] to match experimental results; we also assume that the QDs have the same radius as in [8] to emit at $f_e = 604$ THz). The nanoparticles' shells are assumed to be made of gold, whose relative permittivity ε_3 is described by interpolating the metallic bulk experimental results ε_{JC} from [22] with surface correction as [23, 24]

$$\varepsilon_3 = \varepsilon_{JC} + \frac{\omega_p^2}{\omega(\omega + i\gamma_D)} - \frac{\omega_p^2}{\omega(\omega + i\gamma_F)}. \tag{2}$$

Here $\omega_p = 1.36 \times 10^{16}$ rad s^{-1} is the Drude plasma angular frequency, $\gamma_D = 1.05 \times 10^{14}$ s^{-1} is the Drude damping factor and $\gamma_F = \gamma_D + v_F/(r_3 - r_2)$, with $v_F = 1.39 \times 10^6$ m s^{-1} the Fermi velocity, r_3 the shell outer radius, r_2 the spacer outer radius and $r_3 - r_2$ the metallic thickness. Equation (2) is implemented to avoid underestimation of gold losses when employing the Drude model. We model each nanoshell as a single electric dipole, using the single-dipole approximation (SDA) [1, 2, 25], for which the induced electric dipole moment is $\mathbf{p} = \alpha_{ee}\mathbf{E}^{loc}$, with α_{ee} the nanoshell electric polarizability (we use here the Mie expression reported in [3, 25]) and $\mathbf{E}^{loc}$ the local field acting on it, produced by all the other scattering nanoshells. We determine the modes in the 3D lattice traveling along the z direction with wavenumber $k_z = \beta_z + i\alpha_z$, which may assume real or complex values following the procedure described in [1–3]. In general, two modes with transverse polarization and one mode with longitudinal

polarization with moderately low attenuation constant α_z are present when spatial dispersion is not negligible [2, 26, 27]. However, in all cases treated here, the size of the nanoshells is smaller than that of the nanoparticles in [2, 3] and this implies that spatial dispersion is even lower than the already weak one observed in [2, 3]. Basically, here only one dominant mode, whose electric polarization is in the direction transverse to the mode traveling in the z direction, is propagating. However, a mode with longitudinal polarization with significantly small attenuation constant α_z may appear in a very narrow frequency range, where effective permittivity is vanishing, especially under the low-loss condition treated in this paper. It is therefore one of the purposes of this paper to check this peculiar condition and provide information about the polarization modes able to travel in the composite material. Accordingly, without loss of generality, we consider here the transverse polarization $\mathbf{p} = p_x\hat{\mathbf{x}}$ and the longitudinal polarization $\mathbf{p} = p_z\hat{\mathbf{z}}$. Under these assumptions, the modal wavenumbers are retrieved by solving the scalar equations:

$$A_{xx}(k_z) = 1 - \alpha_{ee}\breve{G}^{\infty}_{xx}(\mathbf{r}_0, \mathbf{r}_0, k_z) = 0, \quad (3)$$

$$A_{zz}(k_z) = 1 - \alpha_{ee}\breve{G}^{\infty}_{zz}(\mathbf{r}_0, \mathbf{r}_0, k_z) = 0, \quad (4)$$

for complex k_z zeros. The terms $\breve{G}^{\infty}_{xx}(\mathbf{r}_0, \mathbf{r}_0, k_z)$ and $\breve{G}^{\infty}_{zz}(\mathbf{r}_0, \mathbf{r}_0, k_z)$ represent the $\hat{\mathbf{x}}\hat{\mathbf{x}}$ and $\hat{\mathbf{z}}\hat{\mathbf{z}}$ components, respectively, of the regularized periodic dyadic Green's function [2] and provide the field contribution evaluated at $\mathbf{r}_0 = x_0\hat{\mathbf{x}}+y_0\hat{\mathbf{y}}+z_0\hat{\mathbf{z}}$ produced by all the nanoshells in the lattice except the one at $\mathbf{r}_0$. To evaluate $\breve{G}^{\infty}_{xx}(\mathbf{r}_0, \mathbf{r}_0, k_z)$ and $\breve{G}^{\infty}_{zz}(\mathbf{r}_0, \mathbf{r}_0, k_z)$ we employ the Ewald method [2, 28–32], for it provides (i) rapid converging summations (i.e. only a handful of summation terms is needed to achieve convergence) and (ii) analytic continuation to the complex k_z plane.

We analyze the physical properties of a lattice whose dimensions are chosen to achieve an ENZ metamaterial around the QD emission frequency when in gain condition: $r_1 = 2$ nm (same radius as in [8]), $r_2 = 4$ nm, $r_3 = 8$ nm, $a = b = c = 21$ nm and a host with relative permittivity $\varepsilon_h = 2.25$. The modal wavenumber for the dominant propagating mode (i.e. the one that contributes mostly to the field in the 3D lattice, as discussed in [2]) with transverse polarization in the case of (i) lossy (i.e. using equation (2)), (ii) lossless (i.e. $\mathrm{Im}[\varepsilon_3] = 0$ artificially imposed) and (iii) loss-compensated lattices is reported in figure 2. At low frequencies, the real part of the modal wavenumber follows a typical dispersion curve which is almost straight. This corresponds to an effective medium slightly denser than the host medium (the light line $\beta_z = k$ is plotted as a black dotted line, where $k = k_0\sqrt{\varepsilon_h}$ is the host wavenumber and k_0 the free space wavenumber) with small attenuation α_z (equal to zero in the lossless case). Then, increasing the frequency, the dispersion curve bends, exhibiting large phase constant β_z (with the largest peak for the lossless case). Thus this mode could be employed in field concentration and imaging applications. Further increasing the frequency, the modal wavenumber experiences a bandgap with a strong attenuation α_z (particularly apparent for the lossless case); finally, at higher frequencies it re-enters a propagation band (except for the lossless case, where

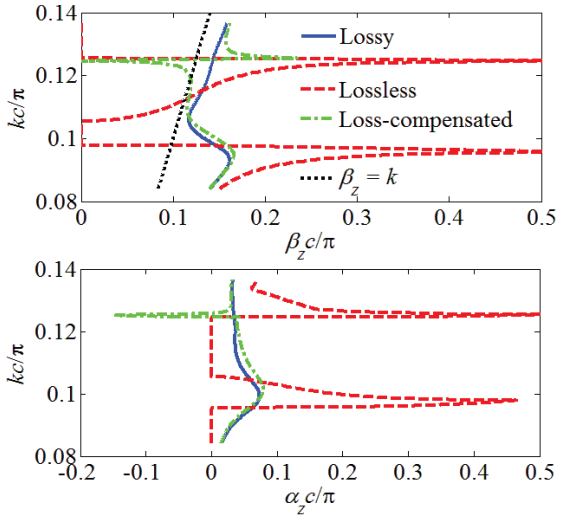

Figure 2. Modal wavenumber dispersion diagram versus frequency for the dominant mode with transverse polarization. (a) Real part and (b) imaginary part of the wavenumber $k_z = \beta_z + \mathrm{i}\alpha_z$ for lossy, lossless and loss-compensated cases.

$\beta_z \approx 0$) with almost constant attenuation. Note that in the loss-compensated case the resonant behavior of the QD in gain condition modifies strongly the dispersion diagram around $kc/\pi \approx 0.125$ (i.e. $f \approx 600$ THz): the adopted QDs provide a large gain (more than required for just loss-compensation). Thus the attenuation constant α_z becomes negative in a narrow frequency band, a symptom of optical amplification (see the discussion in section 3).

Other modes with transverse polarization, dramatically decaying because $\alpha_z \gg k$, and the symptom of a weak spatial dispersion, are present, but their effect can be neglected as discussed in [2, 33]. For example, analogously to what was previously reported in [2], we also find a transversely polarized mode with backward propagation which, however, always has a large attenuation constant $\alpha_z c/\pi > 1$, even in the loss-compensated case and therefore it does not propagate.

The modal wavenumber $k_z = \beta_z + \mathrm{i}\alpha_z$ for the mode with longitudinal polarization in the case of (i) lossy, (ii) lossless (i.e. $\mathrm{Im}[\varepsilon_3] = 0$ artificially imposed) and (iii) loss-compensated lattices is reported in figure 3. In the lossy case, this modal wavenumber is mainly characterized by a large attenuation constant α_z. In the lossless case, instead, this mode has a narrow propagation band with very small attenuation constant α_z at $kc/\pi \approx 0.105$ (i.e. $f \approx 505$ THz), as also described in [2]. Note that this narrow propagation band disappears when considering losses in the metal. At low frequencies, the loss-compensated case follows the lossy one. However, around $kc/\pi \approx 0.125$ (i.e. $f \approx 600$ THz) the adopted QDs provide gain. Thus the attenuation constant α_z is smaller than in the lossy case, in a narrow frequency band. Nevertheless, the normalized attenuation α_z remains larger than 0.5 even at its lower value. In summary, this longitudinal mode in the loss-compensated case is always highly attenuated, even in the very narrow frequency region around $kc/\pi \approx 0.125$, where α_z is still large, and therefore it does not contribute significantly to a field inside the lattice.

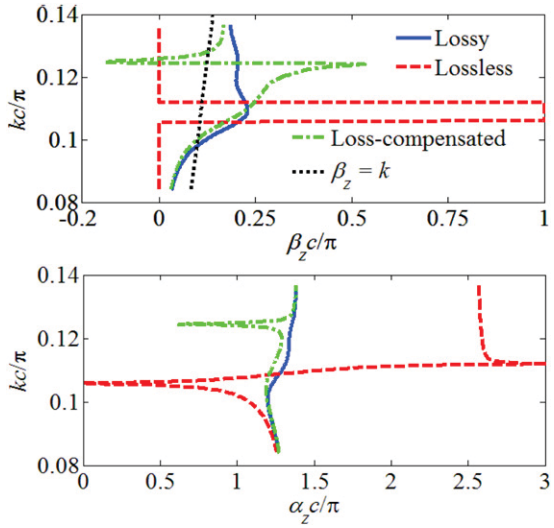

Figure 3. Modal wavenumber dispersion diagram versus frequency with longitudinal polarization. (a) Real part and (b) imaginary part of the wavenumber $k_z = \beta_z + i\alpha_z$, for lossy, lossless and loss-compensated cases.

It is also interesting to note that the propagation constant β_z of this longitudinal mode becomes negative, a symptom of backward propagation, not allowed in standard 3D lattices [2, 26, 27].

3. Loss-compensation and electric permittivity

As previously mentioned, we are interested in generating a loss-compensated ENZ metamaterial as in [3], and also in showing the possibility of achieving large negative values of ε_{eff} with low losses. The results in section 2 have shown that one mode only, with transverse polarization, is able to propagate inside the lattice, and therefore the composite material is now considered for permittivity homogenization. We retrieve the effective permittivity by using three different methods: (i) modal analysis (Mode-SDA), (ii) Maxwell Garnett (MG) homogenization theory and (iii) the Nicolson–Ross–Weir (NRW) retrieval method from reflection R and transmission T of finite thickness structures, here computed using a HFSS full-wave simulation. Note that, when employing MG and NRW methods, it is implicitly assumed that only one propagating mode is dominant, and this has been verified by mode analysis. The comparison among the different methods is performed because their agreement confirms the validity of the homogeneous treatment of the composite material. For brevity, we direct the reader to [2, 3] for a list of references about the MG and NRW methods. Since we deal with losses in the system, both ε_{eff} and n_{eff} are complex valued quantities and can be easily retrieved through modal analysis as $n_{\text{eff}} = k_z/k_0$ and $\varepsilon_{\text{eff}} \approx n_{\text{eff}}^2$, using the results in figure 2. According to NRW, instead, treating the composite slab as a uniform continuous medium with thickness $h = Nc$, with N denoting the number of layers and c the separation between two contiguous layers, the complex

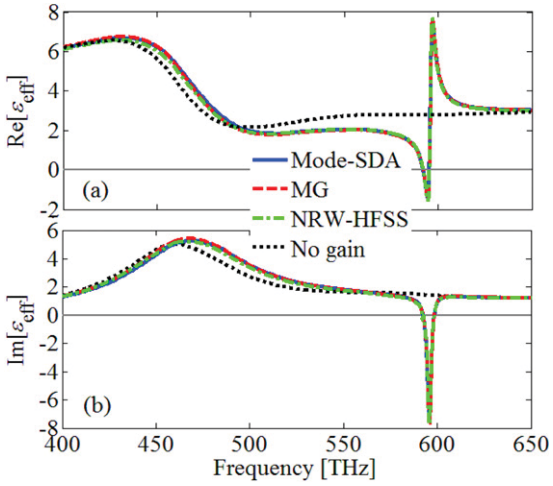

Figure 4. (a) Real and (b) imaginary part of the effective permittivity. The result in the absence of gain is computed using the Mode-SDA method (justified by the agreement of the different methods).

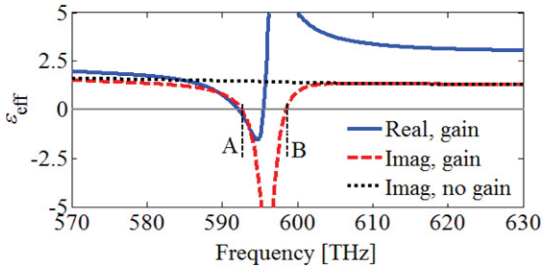

Figure 5. Zoomed ENZ frequency band with and without loss-compensation. The results in the absence and in the presence of gain are computed using the Mode-SDA and the NRW method, respectively (justified by the agreement of the different methods).

effective refractive index can be retrieved as

$$n_{\text{eff}} = \{\pm\cos^{-1}[(1 - R^2 + T^2)/(2T)] + 2\pi q\}/(k_0 h), \quad (5)$$

where q is an integer to be determined. We direct the reader to [2, 3] and references therein for guidelines on how to choose q and $+/-$ in equation (5). Then, one can easily retrieve $\varepsilon_{\text{eff}} \approx n_{\text{eff}}^2$. In general, the NRW solution should be proven to be consistent for varying the number of layers N, as shown in [2] for example. For simplicity in figures 4 and 5 we show only the result with $N = 4$, because results with other N values are found to be in good agreement.

The effective relative permittivity of the homogenized metamaterial discussed in section 2 is reported in figures 4(a) (real part) and (b) (imaginary part) in the presence of gain; the same result in the absence of gain is shown as a dotted black line. The comparison with the different retrieval methods, performed only in the case of gain for clarity of the results, shows very good agreement. Modal analysis usually provides more accurate results than Maxwell Garnett theory around the nanoparticle resonance frequency because it includes all the field retardation effects and all nanoparticle interactions. Since modal analysis is here based on the SDA, full-wave NRW-HFSS is expected to be the most

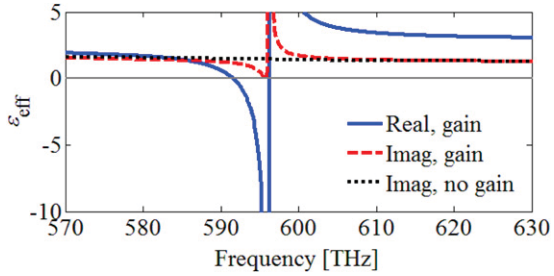

Figure 6. ENZ frequency band with and without loss-compensation by assuming $\gamma_{\text{QD}} \approx 5.26 \times 10^{13}$ s^{-1}. Result computed by using Maxwell Garnett homogenization theory (justified by the agreement of the different methods).

accurate among the three methods for parameter retrieval. However, here the nanoshells and the lattice period are very subwavelength with respect to any guided wavelength. Indeed, the maximum value assumed by the normalized β_z in the lossy and loss-compensated cases reported in figure 2(a) is $\beta_z c/\pi < 0.25$, and therefore $c < \lambda_g/8$, with λ_g being the guided wavelength in the lattice. This implies that the nanoshell dimension is $r_3 \approx c/3 < \lambda_g/24$. For this reason, MG can be used as a powerful tool for the prediction of metamaterial physical properties providing very accurate results.

Note in figure 4 the resonance introduced by the QD around 600 THz. In the absence of gain, the effective permittivity has a large imaginary part and a positive real part around the QD resonance. For clarity, we report in figure 5 a zoomed section of the curves in figures 4(a) and (b) relative to the NRW method. In the frequency range shown before point 'A' (located at around 593 THz) and after point 'B' (located at around 599 THz) absorption losses are compensated (the dashed red curve is lower than the dotted black one, representing the case without gain); moreover, in the region before point 'A', the real part also assumes values very close to zero, proving the feasibility of ENZ properties with low losses. The ENZ behavior is exhibited in a frequency band of about 3 THz, in the range 590.5–593.5 THz. In particular, at around 593 THz the material exhibits no losses ($\text{Im}[\varepsilon_{\text{eff}}] \approx 0$) and $\text{Re}[\varepsilon_{\text{eff}}] \approx -0.2$. In the frequency range between points 'A' and 'B', instead, a negative $\text{Im}[\varepsilon_{\text{eff}}]$ is observed, which means that optical amplification is present in the system. This amplification may involve a natural oscillatory behavior in the system, thus the relation between possible instabilities and an overall gain should be further studied. Nonetheless, this result shows clearly over-compensation capabilities, which means that even less gain could be sufficient for loss-compensation or, vice versa, structures with larger losses could be compensated by the proposed method. These results open up possibilities to loss-compensate efficiently metamaterials by properly tuning the QD resonance frequency and other optical parameters. In the analyzed frequency region in figure 5, before reaching point 'B', the real part of the permittivity also assumes negative values.

In order to avoid optical amplification, and therefore the possible oscillatory behavior described above, we report as

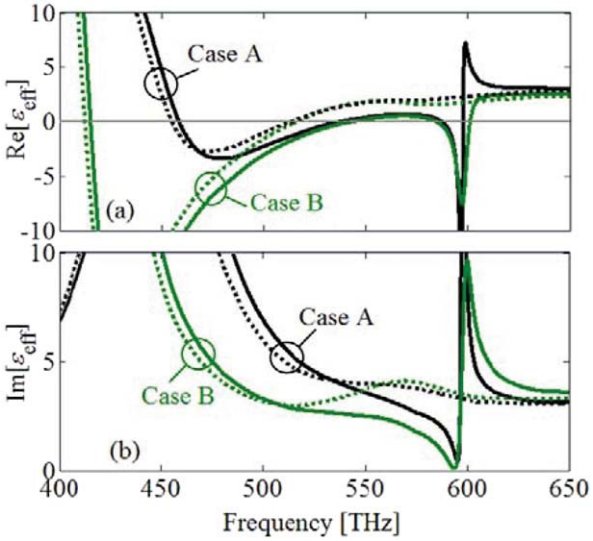

Figure 7. Loss-compensation capabilities varying array physical dimensions. Result computed by using Maxwell Garnett homogenization theory. Solid = with gain; dotted = without gain.

an example in figure 6 the result computed by artificially decreasing the QD broadening parameter to $\gamma_{\text{QD}} \approx 5.26 \times 10^{13}$ s^{-1}. In this case, as shown in figure 6, the loss-compensated metamaterial has $\text{Im}[\varepsilon_{\text{eff}}]$ that never assumes negative values. The metamaterial also exhibits a frequency band where the effective permittivity is large, negative and with very low losses.

Another possible way to avoid the optical amplification described above is by modifying the nanoshell dimensions and nanoshell filling fraction in the composite $f_{\text{vol}} = 4\pi r_3^3/(3abc)$. Two illustrative examples are shown in figure 7, where we analyze the loss-compensation property when varying certain physical dimensions of the 3D lattice as follows, and keeping the others as in section 2: (A) $r_3 = 9$ nm and $f_{\text{vol}} = 44\%$, and (B) $r_2 = 11$ nm, $r_3 = 23$ nm and $f_{\text{vol}} = 50\%$. In both cases, two frequency bands with interesting physical properties can be observed: (i) ENZ behavior in the range 550–590 THz (frequency band of about 40 THz) and (ii) negative permittivity in the range 585–600 THz. We have observed that by varying the filling factor one can tune the permittivity values in the ENZ region. In both cases A and B in figure 7, the presence of gain (solid curves) greatly reduces the value of $\text{Im}[\varepsilon_{\text{eff}}]$ compared to the results without gain (dotted curves), without assuming negative values. Regarding case A, losses have been highly compensated in a wide frequency band, i.e. 530–595 THz, with respect to the case without gain. Case B exhibits a better loss-compensation than Case A in a wider frequency band. Both configurations A and B also exhibit negative $\text{Re}[\varepsilon_{\text{eff}}]$ with very low losses at optical frequencies.

4. Conclusions and final remarks

In conclusion, we have shown the possibility to tailor the effective permittivity to approach virtually almost zero losses in an ENZ frequency band by using small nanoshell

particles, thus creating favorable conditions for a number of applications, including low-threshold nonlinear effects [34]. Moreover, we have observed the generation of negative effective permittivity with low losses to be possible as well. Besides loss-compensation capabilities, the strong gain via QD can provide optical amplification with particular choices of the nanoshell and lattice dimensions, although the relation between possible instabilities and an overall gain should be further studied. These conditions have been obtained by using cores with QDs whose emission band overlaps with that where the 3D lattice exhibits low values of $\mathrm{Re}[\varepsilon_{\mathrm{eff}}]$. In other words, the emission band of the QD cores has been chosen slightly higher than the collective plasmonic resonance frequency of the 3D lattice. One can, however, foresee other possible loss-compensation arrangements that will be studied in future work. For example, QDs can be arranged around a nanosphere or nanoshell as shown experimentally in [35, 36]. That structure would represent a good candidate for loss-compensation studies in optical metamaterials which would, however, require accounting for the nanoshell–QD and QD–QD interactions. The high gain provided by QDs have permitted us to consider nanoshells with very subwavelength dimensions and therefore the electric properties of the composite material can be well described using homogenization techniques.

Acknowledgments

The authors acknowledge partial support from the National Science Foundation (NSF)-CMMI award 1101074. The authors also thank Ansys Inc. for providing HFSS.

References

[1] Steshenko S and Capolino F 2009 Single dipole approximation for modeling collections of nanoscatterers *Theory and Phenomena of Metamaterials* ed F Capolino (Boca Raton, FL: CRC Press) p 8.1
[2] Campione S, Steshenko S, Albani M and Capolino F 2011 *Opt. Express* **19** 26027–43
[3] Campione S, Albani M and Capolino F 2011 *Opt. Mater. Express* **1** 1077–89
[4] Garcia N, Ponizovskaya E V and Xiao J Q 2002 *Appl. Phys. Lett.* **80** 1120–2
[5] Schurig D, Mock J J, Justice B J, Cummer S A, Pendry J B, Starr A F and Smith D R 2006 *Science* **314** 977–80
[6] Pendry J B 2000 *Phys. Rev. Lett.* **85** 3966
[7] Dulkeith E, Morteani A C, Niedereichholz T, Klar T A, Feldmann J, Levi S A, van Veggel F C J M, Reinhoudt D N, Möller M and Gittins D I 2002 *Phys. Rev. Lett.* **89** 203002
[8] Webb K J and Ludwig A 2008 *Phys. Rev.* B **78** 153303
[9] Binetti E, Ingrosso C, Striccoli M, Cosma P, Agostiano A, Pataky K, Brugger J and Curri M L 2012 *Nanotechnology* **23** 075701
[10] Strangi G, De Luca A, Ravaine S, Ferrie M and Bartolino R 2011 *Appl. Phys. Lett.* **98** 251912
[11] De Luca A, Grzelczak M P, Pastoriza-Santos I, Liz-Marzán L M, La Deda M, Striccoli M and Strangi G 2011 *ACS Nano* **5** 5823–9
[12] Xiao S, Drachev V P, Kildishev A V, Ni X, Chettiar U K, Yuan H-K and Shalaev V M 2010 *Nature* **466** 735–8
[13] Gordon J A and Ziolkowski R W 2008 *Opt. Express* **16** 6692–716
[14] Fu Y, Thylén L and Ågren H 2008 *Nano Lett.* **8** 1551–5
[15] Bratkovsky A, Ponizovskaya E, Wang S-Y, Holmstrom P, Thylen L, Fu Y and Agren H 2008 *Appl. Phys. Lett.* **93** 193106
[16] Mackay T G and Lakhtakia A 2009 *Opt. Commun.* **282** 2470–5
[17] Ciattoni A, Marinelli R, Rizza C and Palange E 2011 $|\varepsilon|$-near-zero materials in the near-infrared, arXiv:1107.5540
[18] Zeng Y, Wu Q and Werner D H 2010 *Opt. Lett.* **35** 1431–3
[19] Holmstrom P, Thylen L and Bratkovsky A 2010 *J. Appl. Phys.* **107** 064307
[20] Holmstrom P, Thylen L and Bratkovsky A 2010 *Appl. Phys. Lett.* **97** 073110
[21] Murray C B, Kagan C R and Bawendi M G 2000 *Annu. Rev. Mater. Sci.* **30** 545–610
[22] Johnson P B and Christy R W 1972 *Phys. Rev.* B **6** 4370
[23] Averitt R D, Westcott S L and Halas N J 1999 *J. Opt. Soc. Am.* B **16** 1824–32
[24] Peña O, Pal U, Rodríguez-Fernández L and Crespo-Sosa A 2008 *J. Opt. Soc. Am.* B **25** 1371–9
[25] Bohren C F and Huffman D R 1983 *Absorption and Scattering of Light by Small Particles* (New York: Wiley)
[26] Silveirinha M G 2007 *Phys. Rev.* B **76** 245117
[27] Alù A and Engheta N 2007 *Phys. Rev.* B **75** 024304
[28] Ewald P P 1921 *Ann. Phys. (Berlin)* **64** 253–87
[29] Ham F S and Segall B 1961 *Phys. Rev.* **124** 1786
[30] Stevanoviæ I and Mosig J R 2007 *Microw. Opt. Tech. Lett.* **49** 1353–7
[31] Lovat G, Burghignoli P and Araneo R 2008 *IEEE Trans. Microw. Theory Tech.* **56** 2069–75
[32] Kustepeli A and Martin A Q 2000 *IEEE Microw. Guided Wave Lett.* **10** 168–70
[33] Campione S, Lannebere S, Aradian A, Albani M and Capolino F 2012 *J. Opt. Soc. Am.* B in press
[34] Vincenti M A, de Ceglia D, Ciattoni A and Scalora M 2011 *Phys. Rev.* A **84** 063826
[35] Liu N, Prall B S and Klimov V I 2006 *J. Am. Chem. Soc.* **128** 15362–3
[36] Fanizza E, Malaquin L, Kraus T, Wolf H, Striccoli M, Micali N, Taurino A, Agostiano A and Curri M L 2010 *Langmuir* **26** 14294–300